Biochimica et Biophysica Acta 1848 (2015) 1981–1987

Contents lists available at ScienceDirect

Biochimica et Biophysica Acta

journal homepage: www.elsevier.com/locate/bbamem

Equilibrium binding behavior of magnesium to wall teichoic acid

Kieth J. Thomas III, Charles V. Rice *

Department of Chemistry and Biochemistry, Stephenson Life Sciences Research Center, University of Oklahoma, 101 Stephenson Parkway, Norman, OK 73019, USA

ARTICLE INFO

Article history:
Received 30 November 2014
Received in revised form 20 April 2015
Accepted 6 May 2015
Available online 10 May 2015

Keywords:
Peptidoglycan
Teichoic acid
Magnesium
Homeostasis
Binding

ABSTRACT

Peptidoglycan and teichoic acids are the major cell wall components of Gram-positive bacteria that obtain and sequester metal ions required for biochemical processes. The delivery of metals to the cytoplasmic membrane is aided by anionic binding sites within the peptidoglycan and along the phosphodiester polymer of teichoic acid. The interaction with metals is a delicate balance between the need for attraction and ion diffusion to the membrane. Likewise, metal chelation from the extracellular fluid must initially have strong binding energetics that weaken within the cell wall to enable ion release. We employed atomic absorption and equilibrium dialysis to measure the metal binding capacity and metal binding affinity of wall teichoic acid and Mg^{2+}. Data show that Mg^{2+} binds to WTA with a 1:2 Mg^{2+} to phosphate ratio with a binding capacity of 1.27 μmol/mg. The affinity of Mg^{2+} to WTA was also found to be $41 \times 10^3\ M^{-1}$ at low metal concentrations and $1.3 \times 10^3\ M^{-1}$ at higher Mg^{2+} concentrations due to weakening electrostatic effects. These values are lower than the values describing Mg^{2+} interactions with peptidoglycan. However, the binding capacity of WTA is 4 times larger than peptidoglycan. External WTA initially binds metals with positive cooperativity, but metal binding switches to negative cooperativity, whereas interior WTA binds metals with only negative cooperativity. The relevance of this work is to describe changes in metal binding behavior depending on environment. When metals are sparse, chelation is strong to ensure survival yet the binding weakens when essential minerals are abundant.

1. Introduction

Teichoic acid is a flexible biopolymer found in the cell wall of Gram-positive bacteria. Teichoic acid participates in biofilm production, cell adhesion, cell wall development, cell to cell signaling, host infection, and metal binding [1–6]. Teichoic acid also contains phosphate groups that bind external metal ions and help to keep these ions within the cell wall region [7]. In this fashion, teichoic acid helps to create a reservoir of metals available for homeostatic delivery to the cytoplasm. Wall teichoic acid (WTA) is chemically bound to the peptidoglycan, as opposed to lipoteichoic acid (LTA) that is anchored to the cytoplasmic membrane. The backbone of WTA is composed of glycerol phosphate linkages have branches of D-alanine, *N*-acetylglucosamine, or a hydroxyl group (Fig. 1) [8]. These groups exist in random order and differing amounts dependent on the strain and growth conditions [8,9]. D-Alanine modifications have a pK_a value of 8.42 [10] and thus impart a positive charge to WTA at pH 7. The phosphate groups of teichoic acid have been reported to have a pK_a of 2.1 [11,12], which means that nearly all of the phosphate groups are deprotonated at physiological pH and possess anionic character. Ion pairing between D-alanine and the phosphate is possible, leading to a charge neutral site that should not attract metals [13]. However, this paradigm has been challenged, and the zwitterion is a solvent separated ion pair that does not hinder metal binding [14]. Solid-state NMR studies have shown that Mg^{2+} binding moves the D-alanine farther away from the phosphate and places the D-alanine group in a position that allows for the repulsion of cationic antimicrobial peptides [15].

The importance of teichoic acid in cellular function is demonstrated through genetic mutation studies that remove the ability to synthesis LTA or WTA. The lack of WTA creates a *Bacillus subtilis* cell morphology that has a loss of its rod shape, exhibits swelling, and has increased cell aggregation [16]. The lack of LTA creates a cell morphology that has an increased cell or cell chain length and an increase in cell bending [17]. The morphology reported on LTA deficient mutants is similar to that of Mg^{2+}-deprived cells [18]. Attempts to create double mutants that eliminate both WTA and LTA have shown that the lack of teichoic acids is lethal to cells [17]. The lethality of this combination has been hypothesized to be caused by a lack of divalent cation homeostasis provided by teichoic acid [17]. Here, we report data that characterizes metal binding to WTA as having a Mg^{2+}/P ratio of 1:2 and a binding affinity of $41 \times 10^3\ M^{-1}$ that slowly turns into $1.3 \times 10^3\ M^{-1}$ as the result of reduced electrostatic effects as more Mg^{2+} becomes bound to the sample. The 1:2 Mg^{2+} to phosphate ratio suggest a bridging mode between phosphates. The much lower binding affinity in comparison to that of peptidoglycan [7] also suggests that WTA facilitates movement of metal ions from outside the cell, across the peptidoglycan, and to the cell membrane. These binding affinities and binding modes create a

* Corresponding author.
E-mail address: rice@ou.edu (C.V. Rice).

http://dx.doi.org/10.1016/j.bbamem.2015.05.003
0005-2736/

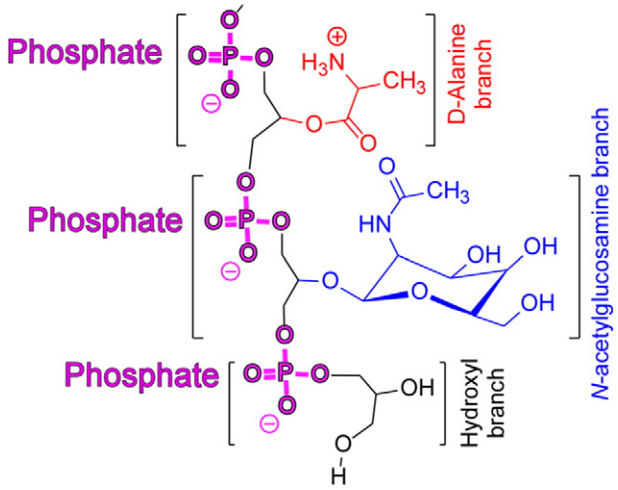

Fig. 1. Polyglycerol backbone of wall teichoic acid. Each polyglycerol phosphate linkage can have different substituents. D-Alanation of WTA is determined by growth conditions such as pH, temperature, and available metal content.

model of ion transport from the environmental milieu to the cytoplasm using teichoic acids. Likewise, these data provide insight into the mechanism of obtaining metals when nutrients are either plentiful or limited.

2. Materials and methods

2.1. Wall teichoic Acid purification

Cell wall samples from *B. subtilis* were grown, harvested, and purified as previously reported [7]. These cell wall samples, containing only peptidoglycan and covalently bound WTA, underwent an additional treatment with 10% TCA (trichloroacetic acid) at 4 °C to remove the WTA. After treatment with TCA, the suspension was centrifuged at 15,000×*g*, and the supernatant was transferred into 1000 MWCO regenerated cellulose dialysis membrane tubing. The dialysis tubing was placed in 2 L of Milli-Q H_2O, which was changed twice at 12-h intervals. Osmotic pressure increased inside the tubing because of the exchange of a large amount of TCA molecules. This required the sample to be lyophilized, re-suspended in a minimal volume of Milli-Q H_2O, and then placed into another 1000 MWCO dialysis membrane section. The dialysis membranes were placed in a 250 mL bath of 0.01 M EDTA at 4 °C overnight to remove residual metal ion concentration. The dialysis membranes were then placed into 2 L of Milli-Q H_2O at 4 °C, and the water bath was changed an additional 6 times during 12-h intervals. The liquid inside the dialysis membrane was transferred to a glass vial and water removed with vacuum lyophilization to produce a white, translucent solid.

2.2. Membrane dialysis procedure

All dialysis experiments were performed in a temperature controlled environment of 4 °C. A known quantity (29.4 mg) of WTA was dissolved in 1 mL of Milli-Q H_2O, placed in a 500 MWCO dialysis membrane, and immersed in 74 mL of Milli-Q H_2O held in a 100 mL glass container with a screw top-lid. The sealed container was allowed to mix in a New Brunswick G24 benchtop shaker (200 rpm) located inside a 4 °C cold room. A temperature of 4 °C was selected to prohibit bacterial growth from outside sources. A concentration gradient was formed on a single sample of WTA due to the time consuming process of WTA purification, and the amount of cell growth that had to be performed to obtain a sufficient amount of WTA. With this procedure, data with varying metal ion concentrations were obtained from a single WTA sample. A 5 mL aliquot of the solution was removed from the glass container every 48 h and the lost volume replaced with 5 mL of a Mg^{2+} solution ($MgCl_2$, 5 ppm). This process was repeated six times to generate 7 samples for analysis of metal ion concentration. For the next 9 samples, removal of 5 mL aliquots was followed by adding 5 ml of a solution with a higher (25 ppm) Mg^{2+} concentration. In this manner, the 25 ppm Mg^{2+} additions create a larger concentration gradient. The Mg^{2+} concentrations of the aliquots from each extraction were analyzed with a Varian SpectraAA 55b Flame Atomic Absorption Spectrophotometer. Without binding, the metal ion concentration should correlate with the standard addition of Mg^{2+} ions. However, because Mg^{2+} binds to WTA, the concentration of Mg^{2+} outside of the dialysis membrane decreases. The amount of Mg^{2+} bound at each equilibrium concentration was determined with a spreadsheet to compare the concentration expected in the absence of binding and the actual concentration. The difference between these values was contributed to metal binding. These quantitative data describe the interaction between Mg^{2+} and WTA. Binding constants from this data were determined with a Scatchard plot. A control containing a dialysis membrane filled with 1 mL of Milli-Q H_2O was subjected through the same process as the WTA sample. Flame AA analysis of the control signified that significant issue with the incomplete equilibrium of metal ions through the membrane and binding of Mg^{2+} to the dialysis membrane did not occur.

2.3. Phosphorus concentration

The purified WTA underwent liquid state ^{31}P NMR analysis to quantify the phosphorus content. The probe was externally calibrated with 0.0485 M triphenyl-phosphate, and one transient scan was taken with a 90° pulse and a 60 s delay time. The gain was set constant for the reference calibration standard and the sample. A 5.9 mg quantity of WTA was dissolved in 750 μL of D_2O and underwent NMR analysis for phosphate concentration. Quantitative analysis of the phosphate content in the WTA sample was performed using the qNMR tools in VnmrJ 3.1, where the integrated peak area for the reference was compared to the sample. A concentration of 21.5 mM of phosphorus was obtained in this analysis. This is equivalent to 2.7 μmol P per mg of WTA and 8.4% phosphorus on a mass percentage. This differs slightly from previous reports of wall teichoic acid from *Staphylococcus aureus* being composed of 6.4% phosphorus [19]. This difference can be attributed to the wall teichoic acid being a polyribitol phosphate polymer, while the *B. subtilis* used in our studies was a polyglycerol phosphate polymer.

2.4. Mg^{2+} binding capacity to WTA

The binding capacity of Mg^{2+} toward WTA can be extrapolated from the Scatchard plot by calculating the amount bound at sufficiently high concentrations (bound vs. unbound = 0). However, slight errors in the affinity constant and its associated slope on the Scatchard plot can produce substantial differences in the estimation of binding capacity. To mitigate this error, the metal binding capacity of WTA was also determined through a simple, one-step method of exposing WTA to a sufficiently high concentration of Mg^{2+}. A known quantity (14.8 mg) of WTA was dissolved in 1 mL of 50 ppm Mg^{2+} solution and placed in a dialysis membrane. The dialysis membrane was then placed in 49 mL of 50 ppm Mg^{2+} solution and allowed to mix in a shaker (4 °C, 200 rpm). After 48 h, the Mg^{2+} concentration outside of the dialysis membrane was examined via Flame AA analysis, and it was discovered that 1.27 μmol of Mg^{2+} was bound per mg of WTA.

3. Results and discussion

The data presented here can be used to elucidate potential binding modes and interactions between metal ions and the cell wall. We now have a better understanding of how Gram-positive bacteria use teichoic acid to control Mg^{2+} uptake depending on the extracellular concentration of metals. This information is essential to understand fundamental biochemical processes that precede metal ion transport through the cell

membrane. By comparing the relative Mg^{2+} binding affinity and capacity with WTA, we observe that the sample initially undergoes possible allosteric changes caused by the addition of metal ions. This is expected since teichoic acid is reported to have a stretched rod confirmation in the absence of metal ions and random coil confirmation develops as the ions in solution increase [20]. During this process, the fraction of metal ions remaining in solution is larger than that observed in the presence of peptidoglycan or peptidoglycan with covalently bound WTA [7]. As the concentration gradient across the dialysis membrane increases, more metal becomes bound. This allows measurement of binding affinities and capacities from flame AA data.

3.1. Positive cooperativity of Mg^{2+} binding to WTA

The binding of Mg^{2+} ions to WTA was measured with atomic absorption spectroscopy which provides a quantitative measurement of metal ion concentration. During equilibrium dialysis, metal ions are bound to WTA within the dialysis bag, and samples for flame AA analysis are taken from the solution outside of the dialysis membrane. Differences between the equilibrium concentration in solution and the known quantity of metal ions added to the sample are used to determine the fraction of metal ions bound to WTA. The data in Fig. 2 show that the serial addition of Mg^{2+} ions leads to increasing amounts of metal bound to WTA. However, the trend is not logarithmic; instead, metal binding appears to increase exponentially. This is in marked contrast to the metal binding behavior within the bacterial cell wall where teichoic acid works in concert with peptidoglycan to chelate metals in a logarithmic fashion [7]. As a result, two models arise for binding metals to WTA. Purified WTA, representing extracellular teichoic acid polymers, initially binds metals with positive cooperativity. However, WTA located within the cell wall which binds metals with negative cooperativity [7].

The equilibrium constant for Mg^{2+} binding to WTA can be found with a Scatchard plot [7]. In this representation (Fig. 3), the positive slope indicates that metal binding has positive cooperativity. This explains why the data in Fig. 2 show that initial binding events make it easier for subsequent metals to bind with WTA. Equilibrium constant (K_A) values are taken from the slope in the Scatchard plot. Unfortunately, the positive slope in Fig. 3 generates a K_A with a negative value and therefore cannot be used to formulate chemical models or comparisons. Nonlinear curve fitting without the use of Scatchard analysis does not take into consideration the cooperative behavior as seen in this system of WTA and Mg^{2+} or the multiple binding sites on a single molecule. We are not aware of any methods to extract precise values of the ever-changing binding affinity constant and can only describe the affinity value as increasing. The positive slope behavior in Scatchard plots has been observed in RNA samples with Mn^{2+} in low ionic strength solutions [21,22]. We believe the initial upward exponential curvature and positive Scatchard plot slope is represented

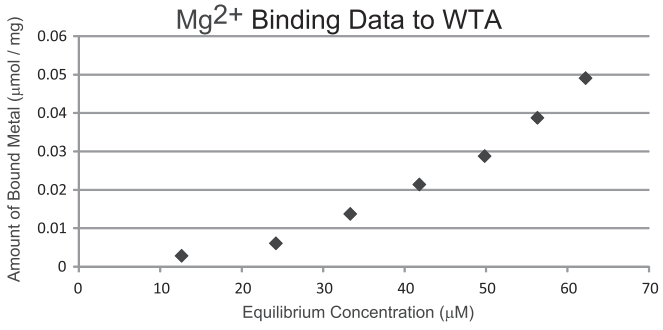

Fig. 2. The binding curve for WTA and Mg^{2+} during the early stages of metal binding. The increase in binding at higher Mg^{2+} concentrations suggests allosteric effects to create stronger binding, perhaps caused by phosphate groups on coming closer together after prior metal binding events.

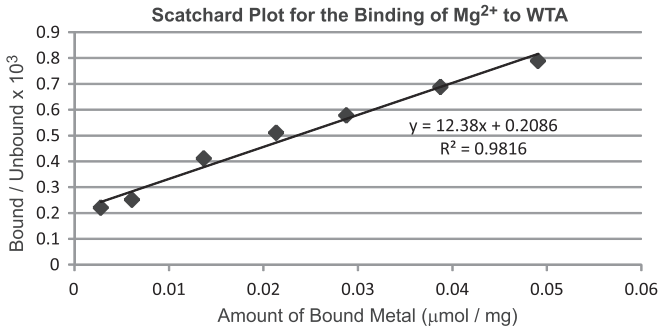

Fig. 3. The Scatchard plot formed from the initial data points of WTA and Mg^{2+} binding shown previously in Fig. 2. Neither binding capacity nor binding affinity parameters can be extracted from these points.

by allosteric effects where the binding of a previous metal ion induces an effect that creates a higher affinity for next binding ions. Such allosteric effects and associated structure changes have been reported for Mn^{2+} binding with tRNA [21]. Teichoic acid has been reported to change structure with the addition of salt [20]. Teichoic acid in dilute buffer or distilled water was reported to have a rigid rod conformation, while salts induced a random coil conformation based on viscosity measurements [20].

Conformational changes within WTA can affect the metal binding affinity by creating new binding sites or bringing the phosphate backbone together. In this scenario, the metal may be chelated in a bridging motif using two phosphate groups. Without metal, the two phosphate groups may be far apart but move together as initial metal binding occurs. This is analogous to the operation of a common zipper. The electrostatic attraction between Mg^{2+} and phosphate groups can be strengthened if two phosphate groups are involved. Similarly to our zipper model, an intermolecular bidentate binding model with Ca^{2+} binding to adjacent phosphate groups on three teichoic acid strands has been proposed [23,24]. It is predicted that divalent metal cations interact and form bridges between peptidoglycan, WTA, LTA, and cell wall proteins [23]. There have been reports on the interaction between metal ions of wall teichoic acid and carboxyl groups on peptidoglycan which signify additional binding mechanisms when attached to the cell wall [25].

Positive cooperativity for metal binding to WTA also suggests that the system may not be at equilibrium. Equilibrium between the inside and outside of the dialysis membrane is reached quickly based on the results of control measurements of water only samples. However, conformational rearrangement of the WTA polymer may be slower. Finding a conformation with the lowest potential energy would require breaking the phosphate-metal-phosphate bridges. The rate of interconversion is unknown. At 4 °C, the sample temperature during the dialysis process, the rate should be slower than observed during cell growth at 37 °C. A simple Arrhenius equation calculation using E_a of 60 kJ/mol, $T_1 = 310$, $T_2 = 277$, gives a rate difference of 0.084 or 12 times slower. Thus, we decided to extend the period of time between collecting flame AA samples. After collecting sample number 7 and adding more metal ions, we waited 21 days to collect sample number 8. To our surprise, the solution equilibrium concentration of Mg^{2+} decreased while the amount of Mg^{2+} bound to WTA increased. The additional 9 μmol/mg of bound Mg^{2+} corresponds directly to the 25 μM drop in solution concentration. These data are informative with regard to the need for additional time for WTA to reach equilibrium, which is remarkable as WTA is a single strand phosphodiester polymer. Likewise, the role of metals in causing rearrangement provides a new chemical perspective on how metals interact with Gram-positive bacteria. When the concentration of metals is low, WTA increases its binding affinity to ensure adequate chelation required for intracellular processes. Yet when metals are abundant, the binding affinity weakens.

The persistence of positive cooperativity over many days suggests that the distribution of metals among all WTA molecules and any structural rearrangements needed to reach their lowest energy conformation are slow processes. This would have the advantage of avoiding dramatic, and perhaps irreversible, reductions of binding affinity in response to short-lived or localized increases in extracellular metal ion concentration.

After allowing 21 days for the sample to reach equilibrium, the time period between subsequent data points was reduced to 48 h, and 25 ppm was added in 5 mL quantities to cause a larger concentration gradient. Here, exponential binding behavior disappears and the data points exhibit linear behavior (Fig. 4). Transformation into a Scatchard plot formulation gives a pattern indicative of negative cooperativity. Electrostatic effects have also been to shown to be responsible for an apparent negative cooperativity in binding studies [22]. The electrostatic effects are responsible for the curvature seen in Fig. 5. As a result, an initial positive cooperativity is observed with a possible reorganization of WTA on metal binding, leading to subsequent negative cooperativity thereafter. Using these later sets of data, it is possible to obtain the binding affinity and metal association equilibrium constants.

3.2. Binding affinity of Mg^{2+} to WTA

The binding affinity of Mg^{2+} to peptidoglycan has been measured [7], $K_A = 1.0 \times 10^6\ M^{-1}$. After the initial positive cooperativity observed with Mg^{2+} binding with WTA, electrostatic effects become more apparent and a concave slope is observed in the Scatchard plot with the last 7 points taken in the experiment (Fig. 5). This behavior is also observed with Mg^{2+} binding to RNA [22,26]. WTA attracts Mg^{2+} ions with a metal binding affinity of $4.07 \times 10^6\ M^{-1}$, which decreases to $1.06 \times 10^3\ M^{-1}$ as seen in Fig. 5.

Both sets of binding data are represented by Fig. 6. A distinct deviation on the curve is observed near the bound region of 0.138 μmol/mg. This data point (#8) was a result from waiting 3 weeks after the final 5 ppm Mg^{2+} addition with first set of data (point #7). The shift in equilibrium concentration and bound Mg^{2+} quantity can be attributed to a potential WTA reorganization to create more binding sites. Incomplete diffusion into the dialysis membrane can be ruled out based a control that went through the same experimental procedure as the sample.

The difference between data points 7 and 8 correlates well with changes in the expected equilibrium concentration and observed equilibrium concentration. The difference in amount bound between points 6 and 7 is 0.0103 μmol/mg and 0.0100 μmol/mg for points 5 and 6. Following the binding trend, we can expect about an additional 0.0103 μmol/mg to be bound, leading to a total approximate bound quantity of 0.059 μmol/mg. However, with point 8, we observe 0.138 μmol/mg being bound to the sample, an increase of 0.079 μmol/mg. Likewise, we also observe a deviation from the trend

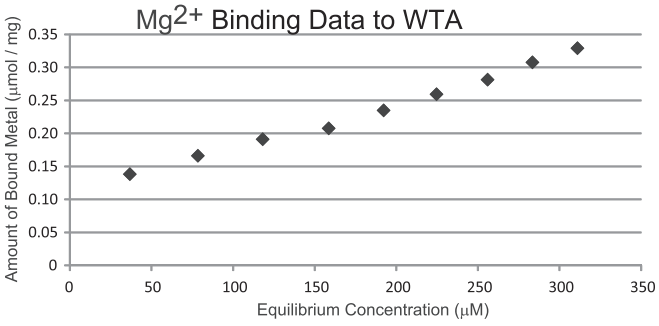

Fig. 4. The binding curve formed from the second set of data points of WTA and Mg^{2+} that were taken 21 days later than the previous set shown previously (Fig. 2). It appears to have a linear relationship.

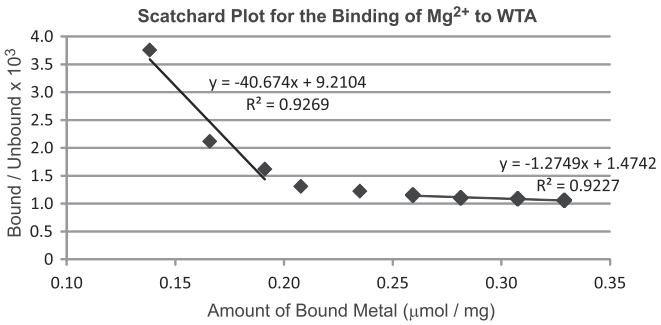

Fig. 5. The Scatchard plot of the metal binding data from Fig. 4 showing the gradually decreasing affinity constant as more metal is added to the system.

in equilibrium concentration, changing from $6.22 \times 10^{-5}\ M^{-1}$ in point 7 to $3.68 \times 10^{-5}\ M^{-1}$ in point 8. A 5 ppm quantity of Mg^{2+} was added after point 7, as in the previous extraction and addition procedure. Taking this into account, we can predict an expected equilibrium concentration around $6.72 \times 10^{-5}\ M^{-1}$. This is a difference of $3.04 \times 10^{-5}\ M^{-1}$ or 2.28 μmol Mg^{2+} in 75 mL of H_2O. With a known sample weight of 29.4 mg, the decrease in equilibrium solution concentration corresponds to a loss of 0.078 μmol Mg^{2+} per mg WTA. This correlates strongly with the observed increase in the fraction of bound metal, 0.079 μmol Mg^{2+} per mg WTA.

3.3. Electrostatic effects and binding capacity

The primary bonding force between metal ions and the phosphate groups of WTA is electrostatic, much like with purified cell wall with peptidoglycan. Electrostatic effects can change, attributed to the structural rearrangement that WTA might undergo initially, plus the decreasing divalent metal ion binding affinity that develops as the molecule becomes less charged. Changes in the electrostatic interaction become apparent after the initial positive cooperativity that could be facilitated by WTA structural changes caused by the initial metal ion binding events. Subsequent negative cooperativity occurs as more metal ions become bound to the biopolymer of WTA and charge neutralization occurs. Equilibrium dialysis measurements with 14.8 mg of WTA in 50 mL of 50 ppm Mg^{2+} solution gave a binding capacity of 1.27 μmol Mg^{2+} per mg WTA. This is equivalent to a Mg^{2+} to P ratio of 0.49:1 based on the phosphorus content per mg of WTA determine by NMR measurements. This supports a bridging chelation mode described earlier with LTA and Cd^{2+} [27].

Teichoic acids account for the majority of the cell's metal binding capacity due to its relative abundance in the cell and binding capacity per milligram. Previous work in our laboratory has shown the effect WTA has on metal binding to the bacterial cell wall [7]. Composed of

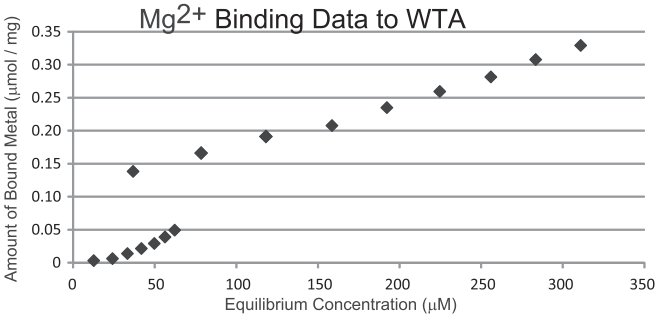

Fig. 6. WTA binding curve for all data points. The first seven data points (amount bound less than 0.05 μmol/mg) were generated with standard additions of a 5 ppm Mg^{2+} solution, whereas the final 9 data points (amount bound is greater than 0.10 μmol/mg) were generated with standard additions of a 25 ppm Mg^{2+} solution.

peptidoglycan and WTA, hydrolysis with trichloroacetic acid separates these two components. After this step, 46% of the cell wall mass remained as an insoluble peptidoglycan component. This supports previous reports that WTA accounts for 20–60% of the total cell wall mass [28]. Cell wall fragments of *B. subtilis* 1A578 containing peptidoglycan and WTA have a Mg^{2+} binding capacity of 0.67 μmol/mg and purified peptidoglycan has a binding capacity of 0.23 μmol/mg at a pH of 5.65. When the binding capacities of peptidoglycan [7] and WTA (this work) are combined with their relative mass percentages, we obtain a theoretical value of 0.73 μmol/mg (0.46×0.23 μmol/mg + 0.54×1.16 μmol/mg). This value compares favorably with the experimental value (0.67 μmol/mg). Thus, WTA has a higher capacity for binding metals than peptidoglycan. These data also reinforce the importance of WTA in metal binding and particular the ability of WTA to extend past the cell wall boundary and chelate metals in extracellular space. This property would also explain why the absence of WTA leads to reduced metal uptake and distorted cell shapes from metal starvation.

3.4. Comparison of metal binding with RNA

WTA is a phosphodiester polymer. RNA is also a phosphodiester polymer and both molecules share metal binding properties. Comparison with previous studies of RNA metal binding can help us understand the initial positive cooperativity mode that changes to negative cooperativity. Both WTA and RNA are polymeric biomacromolecules that bind metal ions. The metal binding behavior in the Scatchard plot of RNA binding Mg^{2+} ions described two classes of binding sites: a group of strongly site bound ions (class I sites) and more weakly bound ions (class II sites) [29]. It has been proposed that each of these modes has a strong coulombic contribution responsible for binding [29]. In addition, ion solvation and other nonelectrostatic contributions are said to be significant [29]. However, this designation of strong and weak sites begins to break down depending on the concentration of monovalent ions and ionic strength, as depicted with divalent metal ions binding with RNA at varying Na^{+} concentrations [22]. This proposed model that designates specific sites as being responsible for the high and low affinity regions is not supported by evidence of "strong" sites de creasing at higher ionic strength values [22]. Nonetheless, the affinities of class I sites for Mg^{2+} binding to tRNA have been reported to be 1×10^{6} M^{-1} [30], 9×10^{4} M^{-1} [31], 2.9×10^{4} M^{-1} [32], and 7.5×10^{4} M^{-1} [26]. Class II sites for Mg^{2+} binding to tRNA were reported to be 1.1×10^{4} M^{-1} [30], 6×10^{3} M^{-1} [31], 4.2×10^{2} M^{-1} [32], and 8.3×10^{2} M^{-1} [26]. The K_A values obtained in work (4.1×10^{4} M^{-1} and 1.3×10^{3} M^{-1}, respectively) correlate well with these values.

3.5. Proposed model of facilitated ion movement to the membrane

WTA extends past the cell wall peptidoglycan and metal ions can interact with WTA individually, or they can interact with the phosphate groups of WTA and carboxyl groups of peptidoglycan simultaneously as seen in Fig. 7. Homeostasis allows metal ions to flow from low affinity binding sites to higher affinity binding sites. In light of the binding association constants for WTA (this work), the binding model proposed for peptidoglycan and cell wall fragments containing peptidoglycan and WTA [7] is incomplete. We suggest that the movement of metal ions from the outer cell wall to the inner cell wall can be viewed in the following manner. Metals originate outside the cell wall in the extracellular fluids, including monovalent and divalent ions. In the case of Mg^{2+} ions, the first interactions with the bacterial cell occur with WTA that extends past the cell wall. Binding to WTA is a bidentate process with an affinity constant of sufficient magnitude to attract metals when necessary while also allowing the metal ions to traverse the phosphodiester backbone. Once the metal ions reach the cell wall, they encounter binding sites formed by peptidoglycan that have a much higher affinity constant. Here, Mg^{2+} ions favor binding to the peptidoglycan component of the cell wall and are desorbed from the external WTA molecules. Nevertheless, WTA is also present within the cell wall and works in concert with peptidoglycan to form the cell wall binding sites. The peptidoglycan itself has a smaller binding capacity but a stronger association constant. However, WTA has a higher binding capacity but a weaker association constant. The result is two types of metal binding interactions within the cell wall. First, strong metal binding by peptidoglycan chelates metal ions required for structural stability and rigidity of the cell wall framework. Because WTA has intimate contact with the peptidoglycan [14], WTA can also contribute the formation of the strong metal binding site. However, WTA can form a cell wall binding site without the need for peptidoglycan. This weaker metal binding environment with a higher metal binding capacity has the

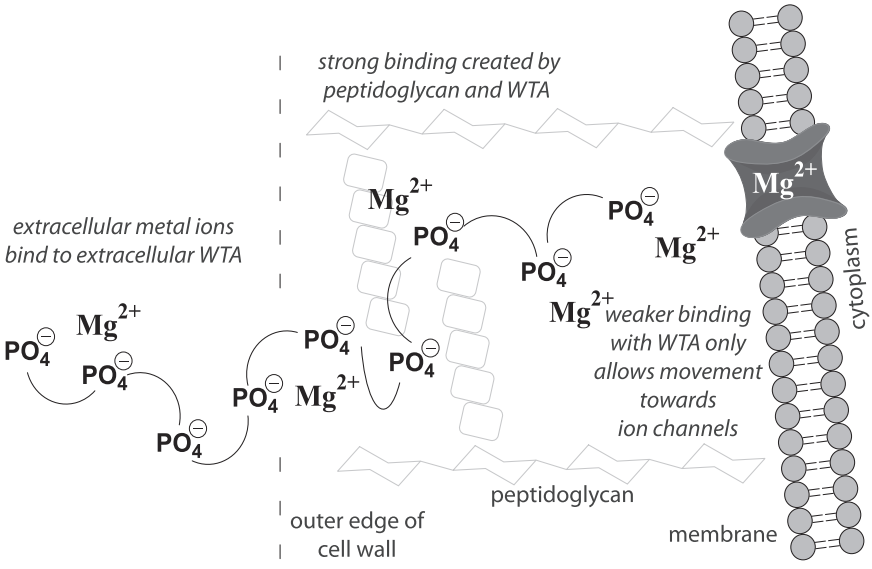

Fig. 7. Potential binding modes between Mg^{2+} with WTA extending past the peptidoglycan layer and WTA inside the peptidoglycan layer. A fragment of the peptidoglycan repeating unit and segment of the wall teichoic acid polymer is shown above. A 1:2 Mg^{2+} to phosphate binding ratio is observed when examining the binding capacity of WTA which gives evidence toward a bridging binding mode between the phosphate groups of WTA. Interactions among the phosphate groups and carboxylate groups of peptidoglycan might also exist within the cell wall.

potential to be the predominate environment for metal ions within the cell wall. In this way, WTA alone can create a reservoir of metal ions that are needed for various intracellular processes. Because the association constant is small, the ions can easily reach the cytoplasmic membrane. There, they can interact with lipoteichoic acid and transmembrane proteins for delivery to the cell interior. Consequently, this metal binding model presents the opportunity to interrupt cellular processes by preventing metal chelation to the phosphodiester backbone of WTA. Agents that have a stronger binding affinity constant than metals would displace the metals from the WTA polymer and perhaps lead to cell death. Effective antibiotics that function in this manner may be difficult to discover as the large fraction of WTA in the cell wall presents the need to large therapeutic doses. However, the innate immune response does include cationic antimicrobial peptides that could function by interacting with WTA to occupy metal binding sites. Antimicrobial peptides have been shown to potentially invoke WTA binding [33]. Current paradigms that describe the function of cationic antimicrobial compounds do not involve the inhibition of metal chelation [34–38]. Work to examine the interactions of WTA, metal ions, and cationic antimicrobial peptides is currently underway.

An important question is whether WTA within the cell wall undergoes structural changes after chelating metals. Previous work in our laboratory has demonstrated the interaction of metals with WTA and peptidoglycan [7]. In these data, there is no indication of positive cooperativity. We cannot imagine a scenario where the rigid peptidoglycan framework undergoes significant structural rearrangement to alter the metal binding site configuration or energetics. To the contrary, it may be possible to WTA to change its structure within the cell wall. Yet the lack of positive cooperativity suggests that the WTA exists in a conformation that is either at its lowest potential energy conformation or interactions between WTA and peptidoglycan prevent WTA rearrangement. In healthy bacterial cells, a reservoir of metals would exist within the cell wall to help WTA obtain its optimal structure. Likewise, WTA outside the cell wall would be immersed in metal rich environment of its biological niche. Metal starvation leads to microbial stress response. An obvious trigger would be the lack of metals in the cytoplasm, but it is possible that additional or earlier triggers are structural changes within WTA from the lack of metals.

4. Conclusion

In this work, we determined the binding affinity and binding capacity of Mg^{2+} to WTA. WTA has a much lower binding affinity for Mg^{2+} compared to the binding affinity of Mg^{2+} to peptidoglycan. At low salt concentrations, Mg^{2+} exhibited an initial binding affinity of $41 \times 10^3\ M^{-1}$ that decreased to $1.3 \times 10^3\ M^{-1}$ as more Mg^{2+} became bound due to electrostatic effects. The binding capacity coupled with the phosphate concentration suggests a 1:2 Mg^{2+} ion to phosphate binding ratio. A binding capacity of 1.27 μmol Mg^{2+} per mg of WTA was determined. WTA and teichoic acids in general are responsible for majority of the Mg^{2+} binding capacity of the cell wall when compared to relative percentage of peptidoglycan in the cell wall sample. We envisage that WTA facilitates the transport of metal ions outside to cell to regions of higher affinity near the cell wall surface. Divalent metal ions can potentially bind in a variety of modes. Metal ions might form any of the following binding modes with the phosphate groups of teichoic acid: monodentate, bidentate, monodentate bridging, bidentate bridging as well as bridging between adjacent strands of WTA. Metal ions can also potentially interact with interaction with both the phosphate groups of WTA and deprotonated carboxyl group of peptidoglycan. In addition, these modes can either be inner-sphere or outer-sphere depending on the hydration state when bound. Due to the chemical similarities of both WTA and LTA being polyglycerol phosphates, it is expected that they would have similar affinity constants. Since WTA can also exist as a polyribitol phosphate polymer, we would expect that the polyribitol version would have a different binding affinity as was reported by previous studies. WTA with a polyribitol phosphate backbone and its associated binding constant have been studied using an equilibrium dialysis method. A binding constant of $0.61 \times 10^3\ M^{-1}$ as well as a Mg^{2+}/P ratio 1:1 was reported [39]. This is in contrast with results of WTA with a polyglycerol phosphate backbone that was reported to have an affinity constant of $2.7 \times 10^3\ M^{-1}$ and Mg^{2+}/P ratio of 1:2 [12]. Our results are in agreement when the salt concentration is high ($1.3 \times 10^3\ M^{-1}$), yet at low salt concentrations, the binding affinity is $41 \times 10^3\ M^{-1}$.

From this and previous work [7], two binding models arise for WTA. Exterior WTA binds metals with positive cooperativity, but after equilibrium is established, metal binding switches to negative cooperativity. Interior WTA binds metals with only negative cooperativity. For both WTA environments, the binding affinity is sufficiently weak to allow metal homeostasis to the cytoplasmic membrane. Yet stronger interactions enable structural integrity from metals binding to peptidoglycan. Our data also show that metal binding behavior changes depending on concentration of Mg^{2+} ions in the immediate cellular environment. Stronger binding ensures survival when metals are sparse yet binding weakens after the requisite metals are obtained from solution.

Transparency document

The Transparency document associated with this article can be found, in online version.

Acknowledgements

This work is supported by the National Institutes of Health (1R01GM090064-01) and the University of Oklahoma.

References

[1] I. Fedtke, D. Mader, T. Kohler, H. Moll, G. Nicholson, R. Biswas, K. Henseler, F. Götz, U. Zähringer, A. Peschel, A *Staphylococcus aureus* ypfP mutant with strongly reduced lipoteichoic acid (LTA) content: LTA governs bacterial surface properties and autolysin activity, Mol. Microbiol. 65 (2007) 1078–1091.
[2] M. Gross, S.E. Cramton, F. Götz, A. Peschel, Key role of teichoic acid net charge in*Staphylococcus aureus* colonization of artificial surfaces, Infect. Immun. 69 (2001) 3423–3426.
[3] M. Vergara-Irigaray, T. Maira-Litrán, N. Merino, G.B. Pier, J.R. Penadés, I. Lasa, Wall teichoic acids are dispensable for anchoring the PNAG exopolysaccharide to the *Staphylococcus aureus* cell surface, Microbiology 154 (2008) 865–877.
[4] C. Weidenmaier, J.F. Kokai-Kun, S.A. Kristian, T. Chanturiya, H. Kalbacher, M. Gross, G. Nicholson, B. Neumeister, J.J. Mond, A. Peschel, Role of teichoic acids in *Staphylococcus aureus* nasal colonization, a major risk factor in nosocomial infections, Nat. Med. 10 (2004) 243–245.
[5] C. Weidenmaier, J.F. Kokai-Kun, E. Kulauzovic, T. Kohler, G. Thumm, H. Stoll, F. Götz, A. Peschel, Differential roles of sortase-anchored surface proteins and wall teichoic acid in *Staphylococcus aureus* nasal colonization, Int. J. Med. Microbiol. 298 (2008) 505–513.
[6] C. Weidenmaier, A. Peschel, Y.Q. Xiong, S.A. Kristian, K. Dietz, M.R. Yeaman, A.S. Bayer, Lack of wall teichoic acids in *Staphylococcus aureus* leads to reduced interactions with endothelial cells and to attenuated virulence in a rabbit model of endocarditis, J. Infect. Dis. 191 (2005) 1771–1777.
[7] K. Thomas III, C. Rice, Revised model of calcium and magnesium binding to the bacterial cell wall, Biometals 27 (2014) 1361–1370.
[8] S. Brown, G. Xia, L.G. Luhachack, J. Campbell, T.C. Meredith, C. Chen, V. Winstel, C. Gekeler, J.E. Irazoqui, A. Peschel, S. Walker, Methicillin resistance in *Staphylococcus aureus* requires glycosylated wall teichoic acids, Proc. Natl. Acad. Sci. 109 (2012) 18909–18914.
[9] A.E. MacArthur, A.R. Archibald, Effect of culture pH on the D-alanine ester content of lipoteichoic acid in *Staphylococcus aureus*, J. Bacteriol. 160 (1984) 792–793.
[10] P. Bernal, M. Zloh, P.W. Taylor, Disruption of d-alanyl esterification of *Staphylococcus aureus* cell wall teichoic acid by the β-lactam resistance modifier (−)-epicatechin gallate, J. Antimicrob. Chemother. 63 (2009) 1156–1162.
[11] R.M.C. Dawson, W.H. Elliott, Data for Biochemical Research, Clarendon Press, 1989.
[12] P.A. Lambert, I.C. Hancock, J. Baddiley, The interaction of magnesium ions with teichoic acid, Biochem. J. 149 (1975) 519–524.
[13] P.A. Lambert, I.C. Hancock, J. Baddiley, Influence of alanyl ester residues on binding of magnesium-ions to teichoic-acids, Biochem. J. 151 (1975) 671–676.
[14] R. Garimella, J.L. Halye, W. Harrison, P.E. Klebba, C.V. Rice, Conformation of the phosphate D-alanine zwitterion in bacterial teichoic acid from nuclear magnetic resonance spectroscopy, Biochemistry 48 (2009) 9242–9249.
[15] M. Kovács, A. Halfmann, I. Fedtke, M. Heintz, A. Peschel, W. Vollmer, R. Hakenbeck, R. Brückner, A functional dlt operon, encoding proteins required for incorporation of

D-alanine in teichoic acids in gram-positive bacteria, confers resistance to cationic antimicrobial peptides in *Streptococcus pneumoniae*, J. Bacteriol. 188 (2006) 5797–5805.
[16] M.A. D'Elia, K.E. Millar, T.J. Beveridge, E.D. Brown, Wall teichoic acid polymers are dispensable for cell viability in *Bacillus subtilis*, J. Bacteriol. 188 (2006) 8313–8316.
[17] K. Schirner, J. Marles-Wright, R.J. Lewis, J. Errington, Distinct and essential morphogenic functions for wall- and lipo-teichoic acids in *Bacillus subtilis*, EMBO J. 28 (2009) 830–842.
[18] M. Webb, The influence of magnesium on cell division: the effect of magnesium on the growth and cell division of various bacterial species in complex media, J. Gen. Microbiol. 3 (1949) 410–417.
[19] J. Baddiley, J. Buchanan, U. Rajbhandary, A. Sanderson, Teichoic acid from the walls of *Staphylococcus aureus* H. Structure of the *N*-acetylglucosaminylribitol residues, Biochem. J. 82 (1962) 439.
[20] R.J. Doyle, M.L. McDannel, U.N. Streips, D.C. Birdsell, F.E. Young, Polyelectrolyte nature of bacterial teichoic acids, J. Bacteriol. 118 (1974) 606–615.
[21] A. Danchin, M. Guèron, Cooperative binding of manganese (II) to transfer RNA, Eur. J. Biochem. 16 (1970) 532–536.
[22] J.L. Leroy, M. Guéron, Electrostatic effects in divalent ion binding to tRNA, Biopolymers 16 (1977) 2429–2446.
[23] F.C. Neuhaus, J. Baddiley, A continuum of anionic charge: structures and functions of D-alanyl-teichoic acids in gram-positive bacteria, Microbiol. Mol. Biol. Rev. 67 (2003) 686–723.
[24] R. Rose, R. Shellis, A. Lee, The role of cation bridging in microbial fluoride binding, Caries Res. 30 (1996) 458–464.
[25] T. Kern, M. Giffard, S. Hediger, A. Amoroso, C.c. Giustini, N.K. Bui, B. Joris, C. Bougault, W. Vollmer, J.-P. Simorre, Dynamics characterization of fully hydrated bacterial cell walls by solid-state NMR: evidence for cooperative binding of metal ions, J. Am. Chem. Soc. 132 (2010) 10911–10919.
[26] M. Bina-Stein, A. Stein, Allosteric interpretation of Mg^{2+} ion binding to the denaturable *Escherichia coli* tRNAGlu2, Biochemistry 15 (1976) 3912–3917.
[27] J.L. Halye, C.V. Rice, Cadmium chelation by bacterial teichoic acid from solid-state nuclear magnetic resonance spectroscopy, Biomacromolecules 11 (2010) 333–340.
[28] I. Hancock, J. Baddiley, Biosynthesis of the bacterial envelope polymers teichoic acid and teichuronic acid, in: A. Martonosi (Ed.), The Enzymes of Biological Membranes, Springer, US 1985, pp. 279–307.
[29] V.K. Misra, D.E. Draper, On the role of magnesium ions in RNA stability, Biopolymers 48 (1998) 113–135.
[30] G. Rialdi, J. Levy, R. Biltonen, Thermodynamic studies of transfer ribonucleic acids. I. Magnesium binding to yeast phenylalanine transfer ribonucleic acid, Biochemistry 11 (1972) 2472–2479.
[31] R. RÖMer, R. Hach, tRNA conformation and magnesium binding, Eur. J. Biochem. 55 (1975) 271–284.
[32] A. Stein, D.M. Crothers, Equilibrium binding of magnesium(II) by *Escherichia coli* tRNAfMet, Biochemistry 15 (1976) 157–160.
[33] T. Koprivnjak, C. Weidenmaier, A. Peschel, J.P. Weiss, Wall teichoic acid deficiency in *Staphylococcus aureus* confers selective resistance to mammalian group IIA phospholipase A2 and human β-defensin 3, Infect. Immun. 76 (2008) 2169–2176.
[34] I. Senyürek, M. Paulmann, T. Sinnberg, H. Kalbacher, M. Deeg, T. Gutsmann, M. Hermes, T. Kohler, F. Götz, C. Wolz, A. Peschel, B. Schittek, Dermcidin-derived peptides show a different mode of action than the cathelicidin LL-37 against *Staphylococcus aureus*, Antimicrob. Agents Chemother. 53 (2009) 2499–2509.
[35] C.Z. Chen, S.L. Cooper, Recent advances in antimicrobial dendrimers, Adv. Mater. 12 (2000) 843–846.
[36] C.L. Friedrich, D. Moyles, T.J. Beveridge, R.E.W. Hancock, Antibacterial action of structurally diverse cationic peptides on gram-positive bacteria, Antimicrob. Agents Chemother. 44 (2000) 2086–2092.
[37] M.A. Gelman, B. Weisblum, D.M. Lynn, S.H. Gellman, Biocidal activity of polystyrenes that are cationic by virtue of protonation, Org. Lett. 6 (2004) 557–560.
[38] N.M. Milović, J. Wang, K. Lewis, A.M. Klibanov, Immobilized *N*-alkylated polyethylenimine avidly kills bacteria by rupturing cell membranes with no resistance developed, Biotechnol. Bioeng. 90 (2005) 715–722.
[39] J.E. Heckels, P.A. Lambert, J. Baddiley, Binding of magnesium-ions to cell-walls of *Bacillus-subtilis*-W23 containing teichoic-acid or teichuronic acid, Biochem. J. 162 (1977) 359–365.